the radar images. Thus, in contrast to other regions on Venus, where craters seem to imply a quiescent surface history, this portion of the planet appears to have experienced tectonic modification at least as severe as that seen on Mars, and perhaps similar to that associated with terrestrial plate tectonic activity.

Summary. The recent radar images of Venus suggest the following features and interpretations.

1) Circular features in some areas may be of impact origin. If so, their existence implies relatively quiescent surface modification processes.

2) A great trough-like depression near 0°,76°W suggests extensional tectonic activity.

3) Two types of central volcanism (one forming single large constructs and one forming clusters of smaller peaks) are suggested by the interpretation of features near 10°S,40°W and 10°S,10°E.

4) A region of mountainous terrain and sharply defined lineaments may indicate compressional tectonism, although extension could also explain these features.

5) Large expanses of moderate or high reflectivity suggest bouldery surfaces, a point well illustrated by images of the surface of Venus returned by the Soviet spacecraft Venera 9 and Venera 10.

In conclusion, the radar images in part seem to indicate that some regions of Venus have remained little altered since a period of intense bombardment similar to that recorded by the many large impact craters on the moon, Mercury, and Mars. On the other hand, there is evidence in other regions that Venus has been a geologically active planet, forming diverse landforms, and perhaps rivaling the earth in the breadth of features portrayed on its surface. The possibility of studying features remarkably like those on the earth make Venus an exciting candidate for future exploration.

MICHAEL C. MALIN
R. STEPHEN SAUNDERS
Planetology and Oceanography Section, Jet Propulsion Laboratory, California Institute of Technology, Pasadena 91103

References and Notes

1. H. C. Rumsey, G. A. Morris, R. R. Green, R. M. Goldstein, *Icarus* **22**, 1 (1974).
2. R. M. Goldstein, *Eos* **56**, 388 (1975); _____, R. R. Green, H. Rumsey, *J. Geophys. Res.* **81**, 4807 (1976).
3. On 23 and 28 December 1973, 13 and 20 January 1974, and 1, 18, and 27 February 1974, Venus was observed by using the Goldstone 64-m antenna to transmit a 400-kw, continuous-wave, 12.6-cm signal, and both the 64-m and a 26-m antenna to receive the echoes (*1*, *2*). The interferometer baseline was 22 km. Each Doppler–time delay cell was approximately 10 km square. A brief discussion of the radar technique used to acquire the data shown here is presented in (*4*).
4. The radar techniques used to produce the images discussed here analyze the returned echo in time, frequency, and power. In the application of these techniques, the reflected signals are "chopped" in time slices as they are received, forming collar-like zones concentric with the subradar point [see figure 1 in (*5*) and figure 2, a and b, in (*6*)]. The more rapidly the signal is sampled, the smaller the width and the higher the resolution. These zones are generally called time delay or range gates. Frequency analyses of the range-gated echoes, which capitalize on Doppler shifts associated with planetary rotation, provide a second spatial coordinate. Lines of equal Doppler shift (both positive and negative) are circles parallel to the plane containing the rotation axis and the subradar point and are thus seen edge-on by the radar as lines parallel to the rotation axis. Again, the finer the frequency slices, the higher the resolution. High resolution is inhibited, however, by the fact that time delay and frequency slices must be weighed against the integration time and area required to achieve a reasonable signal-to-noise ratio for the returned echoes. Three problems arise from these observational techniques. (i) A given pair of time-delayed and Doppler-shifted values can be mapped to two locations symmetrically above and below the radar equator defined by the plane perpendicular to the rotation axis and containing the subradar point [see figure 2 in (*6*)]. This north-south ambiguity can be eliminated by two techniques. The first is a form of single-antenna "stereo" viewing and multiple-antenna "interferometry." The apparent stereo angle is acquired over many days as the subradar point moves across the surface of Venus in response to terrestrial and venusian rotational and orbital motions. By viewing the echoes from multiple "positions," and watching for variations in the signal strength of individual cell returns as the subradar point moves north or south, it is possible to remove most of the major effects of the ambiguity (*5*, *7*). In the second technique two signals (received by two antennas used as an interferometer), which are shifted in phase because of the separation of the antennas, are combined to produce contours of constant phase shift. These contours can be used to alleviate the north-south ambiguity, since the two cells with the same Doppler and time delay have phases of opposite sign (*1*, *8*). (ii) The so-called poison points (*1*) result when, because of insufficient rotation of the interferometer baseline, it is not possible to distinguish null points of integer phase, which are seen most prominently in the altimetry maps as bands parallel to the radar equator. (iii) Finally, because the time delay and Doppler coordinates are parallel at, and perpendicular to, the radar equator [see figure 2 in (*6*)], and because of the large size of the front cap range ring (*1*), the data from these portions of the Venus radar images have been suppressed. Thus each image contains a black zone along the radar equator, called the runway (*1*).
5. R. M. Goldstein and H. Rumsey, *Science* **169**, 974 (1970).
6. S. Zohar and R. M. Goldstein, *Astron. J.* **79**, 85 (1974).
7. R. M. Goldstein and H. C. Rumsey, *Icarus* **17**, 699 (1972).
8. A. E. E. Rogers and R. P. Ingalls, *Radio Sci.* **5**, 425 (1970).
9. Thus, regional slopes in the direction of the subradar point having the same inclination as the radial distance in degrees will appear brightest. For example, if there were a domical hill 2° from the center of the image, that part of the hill having a local slope of 2° toward the image center would appear brightest. Conversely, the darker part of the feature would be that part with the greatest slope away from the image center. Shadows occur when the slope away from the subradar point exceeds the complement of the angular offset.
10. R. S. Saunders and M. C. Malin, *Geol. Rom.*, in press.
11. G. G. Schaber and J. M. Boyce, *Moon*, in press.
12. R. P. Sharp, *J. Geophys. Res.* **78**, 4063 (1973).
13. W. K. Hartmann, *Icarus* **19**, 550 (1973).
14. P. Masson, *ibid.* **30**, 49 (1977).
15. B. H. Baker, P. A. Mohr, L. A. J. Williams, *Geol. Soc. Am. Spec. Pap. 136* (1973).
16. M. Carr, *J. Geophys. Res.* **78**, 4049 (1973).
17. _____, in *Proceedings of an International Colloquium on Planetary Geology*, Rome, September 1975.
18. H. S. Colton, *Mus. North. Ariz. Bull. 10* (1950).
19. P. M. Vincent, in *African Magmatism and Tectonism*, T. N. Clifford and I. G. Glass, Eds. (Hafner, Darien, Conn., 1970), p. 301.
20. J. F. Dewey and J. M. Bird, *J. Geophys Res.* **75**, 2625 (1970).
21. L. Wright, *Geology* **4**, 489 (1976).
22. This report presents the results of one phase of research carried out at the Jet Propulsion Laboratory under contract NAS 7-100, sponsored by the Planetology Program Office, Office of Space Science, National Aeronautics and Space Administration.

28 December 1976

Photoassisted Electrolysis of Water by Visible Irradiation of a *p*-Type Gallium Phosphide Electrode

Abstract. *Photoelectrolytic decomposition of water with visible irradiation is demonstrated in a cell made of* p*-type gallium phosphide as the cathode and platinum as the anode. A maximum energy conversion efficiency of 0.1 percent is achieved with an external bias of 1.3 volts. The stability of the electrode is demonstrated, and the results are discussed in terms of a composite energy diagram.*

Of the various schemes to convert solar energy into chemical energy, photoassisted electrolysis of water is beginning to show promise as a practical method. Photoassisted electrolysis of water by ultraviolet irradiation of *n*-type semiconductor electrodes has been demonstrated in a number of systems (*1*, *2*). The significance of a photoelectrolytic device for the conversion and storage of solar energy was emphasized in a number of publications during the last few years (*3*). Such a system must fulfill three basic requirements: (i) it must bring about the light-

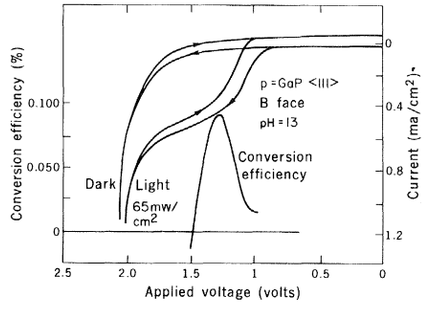

Fig. 1. Current-voltage and conversion efficiency–voltage diagrams for a cell made of Zn-dopped GaP, $\langle \bar{1}\bar{1}\bar{1} \rangle$ as the cathode and Pt foil as the anode. The electrolyte was $10^{-2}M$ NaOH + $0.5M$ Na_2SO_4. The light source was an attenuated, water-filtered, 75-watt Xe lamp.

induced decomposition of water to H_2 and O_2; (ii) it must exhibit catalytic behavior, with water being the only consumed product; and (iii) it must have positive energy conversion efficiency for solar radiation.

We have found that an electrochemical cell with *p*-type GaP as the cathode and Pt foil as the anode meets all three requirements. This cell configuration differs from earlier cells (*4*) in which *n*-TiO_2 and *p*-GaP electrodes were used. The current-voltage behavior of a Pt *p*-type GaP cell is shown in Fig. 1. The onset of the dark electrolysis occurs at about 1.7 volts, whereas the onset of the light-assisted electrolysis occurs at about 1.0 volt and saturates at about 1.4 volts. The current saturation level is proportional to the light intensity. When current flowed in the system, a strong evolution of H_2 on the cathodic-biased GaP electrode and of O_2 on the Pt electrode was observed.

The energy conversion efficiency of radiant energy into chemical energy, η, was calculated according to the following formula (*2*):

$$\eta = \frac{I_c\,(1.48 - V) \times 100}{I_a}$$

where I_c is the current flowing in the system (in milliamperes per square centimeter), V is the cathodic bias on the GaP electrode, and I_a is the intensity of the light incident on the sample (in milliwatts per square centimeter). The 1.48 term is derived from the heat of formation of water at 25°C. Therefore, with respect to the conversion of solar energy into chemical energy, the efficiency will be positive for applied voltages less than 1.48 volts. This means that for an applied voltage of less than 1.48 volts, the energy of combustion of the photolytically formed H_2 will be greater than the electrical energy supplied to the photoelectrolysis system. Of course, any practical system for solar energy conversion will have to take into account the associative efficiencies of the subsequent use of the H_2; we are concerned here only with the chemical energy available in the H_2. The conversion efficiency, for a water-filtered, 75-watt Xe light source, as a function of the applied voltage, is also shown in Fig. 1. The efficiency peaks at ~ 0.1 percent for a 1.3-volt bias. The *p*-type GaP cathode was a $\langle \bar{1}\bar{1}\bar{1} \rangle$ surface of a Zn-doped crystal grown by a liquid encapsulation method (*5*) with a carrier concentration of 10^{18} holes per cubic centimeter and a resistivity of 0.01 ohm-cm. This resistivity is much too low to account for the photoeffect we see in terms of simple photoconductivity.

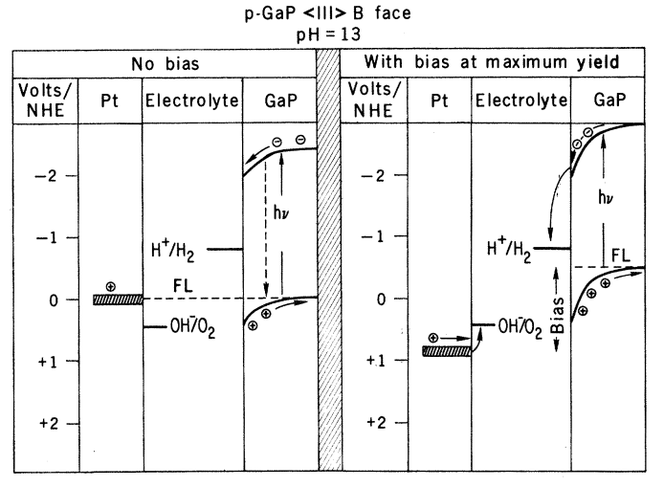

Fig. 2. Energy diagram for the combined cell under no bias and no photoelectrolysis conditions and under the conditions when the maximum conversion efficiency was obtained. All energies are with respect to normal hydrogen electrolyte. Abbreviations: *NHE*, normal hydrogen electrolyte; *FL*, Fermi level.

We checked the stability of the electrode by passing 100 coulombs of electricity, using a high-intensity light source which produced an average current density of 5 ma/cm². Under these conditions the sample did not show any signs of dissolution or corrosion. The mirrorlike surface showed no visible alteration, and no measurable change in sample weight was found; atomic absorption spectroscopy revealed that less than 1.5×10^{-7} mole of Ga was present in the 0.5*M* H_2SO_4 electrolyte. We did not observe any significant changes in performance with changing *p*H. However, significant changes were observed as a function of crystal preparation, doping level, surface condition, and orientation.

The current-potential curves of the GaP electrode and the Pt electrode were measured against standard calomel electrodes. From this information and the flat-band potentials measured by Memming (*6*), the combined energy diagram given in Fig. 2 was constructed.

It can be seen from Fig. 2 that the bias is needed, both to lower the Fermi level of the Pt electrode below its overpotential for O_2 evolution and to increase the band-bending of the GaP. The fact that it is necessary to increase the band-bending from about 0.5 to about 1.0 volt in order to achieve photocurrent saturation indicates that the GaP crystals used in these experiments had very poor diffusion lengths for the minority carriers. Current saturation would be expected to occur at about 1.0 volt of bias for higher-quality GaP. Similar studies were made on *p*-type GaAs, InP, and GaAlAs, but all of these required higher applied voltage for photoelectrolysis. Clearly, more efficient devices, based on *p*-type semiconductor electrodes, will require flat-band potentials that are more positive than the O_2 electrode and smaller band-bending necessary to achieve the light-limiting charge separation.

Since we have been able to determine the combined energy diagram for the Pt *p*-type GaP system, we can estimate the theoretical limits of this system for GaP electrodes with a quantum efficiency for charge separation of unity with the band-bending at zero bias condition. For Air Mass 2 solar irradiance, I_a = 74 mw/cm²; I_c should be about 7.5 ma/cm² (*7*) and V should be about 1 volt in order to produce a conversion efficiency of about 4 to 5 percent.

MICHA TOMKIEWICZ*
JERRY M. WOODALL
T. J. Watson Research Center, International Business Machines Corporation, Yorktown Heights, New York 10598

References and Notes

1. A. Fujishima and K. Honda, *Nature (London)* **238**, 37 (1972); A. Fujishima, K. Kohayakawa, K. Honda, *J. Electrochem. Soc.* **122**, 1437 (1975); M. S. Wrighton, D. S. Ginley, P. T. Wolczanski, A. B. Ellis, D. L. Morse, A. Linz, *Proc. Natl. Acad. Sci. U.S.A.* **72**, 1518 (1975); M. S. Wrighton, D. L. Morse, A. B. Ellis, D. S. Ginley, H. B. Abrahamson, *J. Am. Chem. Soc.* **98**, 44 (1976); J. G. Mavroides, D. I. Tchernev, J. A. Kafalas, D. F. Kolesar, *Mater. Res. Bull.* **10**, 1023 (1975); T. Oshnishi, Y. Nakato, H. Tsubomura, *Ber. Bunsenges. Phys. Chem.* **79**, 523 (1975); K. L. Hardee and A. J. Bard, *J. Electrochem. Soc.* **122**, 139 (1975); W. Gissler, P. L. Lensi, S. Pizzini, *J. Appl. Electrochem.* **6**, 9 (1976); J. Keeney, D. H. Weinstein, G. M. Haas, *Nature (London)* **253**, 719 (1975); J. G. Mavroides, J. A. Kafalas, D. F. Kolesar, *Appl. Phys. Lett.* **28**, 241 (1976).
2. A. J. Nozik, *Nature (London)* **257**, 383 (1975).
3. M. D. Archer, *J. Appl. Electrochem.* **5**, 17 (1975); G. Stein, *Isr. J. Chem.* **14**, 213 (1975).
4. H. Yoneyama, H. Sakamoto, and H. Tamura [*Electrochim. Acta* **20**, 341 (1975)] and A. J. Nozik (in preparation) have reported the use of *n*-TiO_2, *p*-GaP heterotype cells for photoelectrolysis.
5. S. É. Blum, R. J. Chicotka, B. K. Bischoff, *J. Electrochem. Soc.* **115**, 324 (1968).
6. R. Memming, *ibid.* **116**, 785 (1969).
7. H. J. Hovel, in *Semiconductors and Semimetals: Solar Cells*, R. K. Willardson and A. C. Beer, Eds. (Academic Press, New York, 1975), vol. 11.

* Present address: Union Carbide Corporate Research Laboratory, Tarrytown Technical Center, Tarrytown, New York 10591.

20 May 1976; revised 12 November 1976